

MSUHEP-50727 DOE-ER40757-069 CPP-95-12

# Production of pseudoscalar Higgs-bosons in $e\gamma$ collisions

Duane A. Dicus

*Center for Particle Physics and Department of Physics  
University of Texas, Austin, Texas 78712*

Wayne W. Repko

*Department of Physics and Astronomy  
Michigan State University, East Lansing, Michigan 48824*

(February 1, 2008)

## Abstract

We investigate the production of a pseudoscalar Higgs-boson  $A^0$  using the reaction  $e\gamma \rightarrow eA^0$  at an  $e\bar{e}$  collider with center of mass energy of 500 GeV. Supersymmetric contributions are included and provide a substantial enhancement to the cross section for most values of the symmetry breaking parameters. We find that, despite the penalty incurred in converting one of the beams into a source of backscattered photons, the  $e\gamma$  process is a promising channel for the detection of the  $A^0$ .

13.85.Qk, 14.80.Er, 14.80.Gt

Typeset using REVTEX

## I. INTRODUCTION

The Higgs sector in supersymmetric extensions of the standard model contains charged Higgs-bosons as well as additional neutral Higgs-bosons [1]. Among the latter is a pseudoscalar particle usually denoted  $A^0$ . In this paper, we calculate the production cross section for the  $A^0$  in the process  $e\gamma \rightarrow eA^0$ . Contributions to this process arise from triangle and box diagrams. The triangle contributions consist of diagrams in which the  $A^0$  and photon are on-shell external particles and the remaining particle is a virtual photon or  $Z^0$  in the  $t$ -channel. Since  $t = 0$  is in the physical region, the photon pole contribution dominates the  $Z^0$  pole contribution in this set of diagrams [2]. Moreover, because of the off-diagonal structure of the  $A^0$  couplings to other bosons, the particles in the loop are either quarks, leptons or charginos. Here, we present the top quark, bottom quark, tau lepton and the two chargino contributions to the photon pole amplitude.

The box diagrams have a more complex particle structure, with leptons, charginos, neutralinos and scalar leptons in the loops. Like the  $Z^0$  pole, these diagrams are non-singular at  $t = 0$ , and should not contribute a sizable correction to the photon pole terms. They are not included in the present calculation.

## II. THE CROSS SECTION FOR $A^0$ PRODUCTION

The amplitude for the production of an  $A^0$  of momentum  $k'$  and an  $e$  of momentum  $p'$  in the collision of an  $e$  of momentum  $p$  and a  $\gamma$  of momentum  $k$  and polarization  $\varepsilon_\lambda(k)$  by the exchange of a  $\gamma$  in the  $t$ -channel is

$$\mathcal{M} = \frac{4i\alpha^2}{\sin\theta_W m_W} \bar{u}(p') \gamma_\mu u(p) \frac{\mathcal{A}_\gamma(t)}{t} \varepsilon_{\mu\nu\alpha\beta} \varepsilon_\nu(k) (p - p')_\alpha k_\beta , \quad (1)$$

where  $t = -(p - p')^2$ , and

$$\mathcal{A}_\gamma(t) = \left[ -3 \left( \frac{2}{3} \right)^2 m_t^2 \cot\beta C_0(t, m_A^2, m_t^2) - 3 \left( -\frac{1}{3} \right)^2 m_b^2 \tan\beta C_0(t, m_A^2, m_b^2) \right] \quad (2)$$

$$\begin{aligned}
& -(-1)^2 m_\tau^2 \tan \beta C_0(t, m_A^2, m_\tau^2) + 2m_W m_1 g_{11} C_0(t, m_A^2, m_1^2) \\
& + 2m_W m_2 g_{22} C_0(t, m_A^2, m_2^2) \Big] ,
\end{aligned}$$

Here,  $m_t$  and  $m_b$  are the top and bottom quark masses,  $m_\tau$  is the tau lepton mass,  $m_1$  and  $m_2$  are the chargino masses,  $m_W$  is the  $W$  mass and  $\tan \beta$  is a ratio of vacuum expectation values [1]. The chargino coupling constants  $g_{11}$  and  $g_{22}$  depend on the elements of two  $2 \times 2$  unitary matrices  $U$  and  $V$  which diagonalize the chargino mass matrix  $X$ , where [3]

$$X = \begin{pmatrix} M & \sqrt{2}m_W \sin \beta \\ \sqrt{2}m_W \cos \beta & \mu \end{pmatrix}, \quad (3)$$

and are chosen to ensure that  $m_1$  and  $m_2$  are positive. For illustrative purposes, we assume that the symmetry breaking parameters  $M$  and  $\mu$  are real and consider two cases:  $M\mu > m_W^2 \sin 2\beta$  and  $M\mu < m_W^2 \sin 2\beta$ . The couplings in these cases are

$$g_{11} = \frac{m_W}{m_1^2 - m_2^2} (m_2 + m_1 \sin 2\beta), \quad g_{22} = -\frac{m_W}{m_1^2 - m_2^2} (m_1 + m_2 \sin 2\beta), \quad (4)$$

for  $M\mu > m_W^2 \sin 2\beta$ , and

$$g_{11} = \frac{m_W}{m_1^2 - m_2^2} (-m_2 + m_1 \sin 2\beta), \quad g_{22} = -\frac{m_W}{m_1^2 - m_2^2} (-m_1 + m_2 \sin 2\beta), \quad (5)$$

for  $M\mu < m_W^2 \sin 2\beta$ . Notice that, these couplings are symmetric in  $m_1$ ,  $m_2$  and, unlike the  $A^0$ -top coupling, there is no enhancement factor of  $m_{1,2}/m_W$  [4]. We take  $m_1 > m_2$ . Due to the reality of  $M$  and  $\mu$ ,  $m_1$  and  $m_2$  in Eqs. (4, 5) are subject to certain constraints discussed below [5]. The scalar function  $C_0(t, m_A^2, m^2)$  is [6]

$$C_0(t, m_A^2, m^2) = \frac{1}{i\pi^2} \int d^4 q \frac{1}{(q^2 + m^2) ((q + p - p')^2 + m^2) ((q + p - p' + k)^2 + m^2)}. \quad (6)$$

Since one of the external particles is a photon, this function can be expressed in terms of inverse trigonometric or hyperbolic functions [1,7] as

$$C_0(t, m_A^2, m^2) = \frac{1}{(t - m_A^2)} \left( C\left(\frac{m_A^2}{m^2}\right) - C\left(\frac{t}{m^2}\right) \right), \quad (7)$$

where

$$C(\beta) = \int_0^1 \frac{dx}{x} \ln(1 - \beta x(1-x) - i\varepsilon) \quad (8)$$

$$= \begin{cases} 2 \left( \sinh^{-1} \left( \sqrt{-\frac{\beta}{4}} \right) \right)^2 & \beta \leq 0 \\ -2 \left( \sin^{-1} \left( \sqrt{\frac{\beta}{4}} \right) \right)^2 & 0 \leq \beta \leq 4 \\ 2 \left( \cosh^{-1} \left( \sqrt{\frac{\beta}{4}} \right) \right)^2 - \frac{\pi^2}{2} - 2i\pi \cosh^{-1} \left( \sqrt{\frac{\beta}{4}} \right) & \beta \geq 4 \end{cases} . \quad (9)$$

The cross section is given by

$$\frac{d\sigma(e\gamma \rightarrow eA_0)}{d(-t)} = \frac{1}{64\pi s^2} \sum_{\text{spin}} |\mathcal{M}|^2 , \quad (10)$$

and we have

$$\sum_{\text{spin}} |\mathcal{M}|^2 = \frac{\alpha^4}{\sin^2 \theta_W m_W^2} (s^2 + u^2) \frac{|\mathcal{A}_\gamma(t)|^2}{(-t)} , \quad (11)$$

where  $s = -(p+k)^2$  and  $u = -(p'-k)^2$ . The presence of the  $1/t$  in Eq. (11) means it is necessary to introduce a cutoff in the calculation of the total cross section. One approach to obtaining a finite cross section is use the effective photon or Weizsäcker-Williams approximation for the exchanged photon [8]. Here, we integrate the exact amplitude and impose an angular cutoff. The expression for the total cross section is

$$\sigma_{e\gamma \rightarrow eA^0}(s) = \frac{\alpha^4}{64\pi \sin^2 \theta_W m_W^2} \int_{\eta(s-m_A^2)}^{(s-m_A^2)} \frac{dy}{y} \left( 2 - 2 \frac{(m_A^2+y)}{s} + \frac{(m_A^2+y)^2}{s^2} \right) |\mathcal{A}_\gamma(-y)|^2 , \quad (12)$$

where  $\eta$  is an angular cutoff. We investigated the effect of varying  $\eta = \sin^2(\theta_{\min}/2)$  by comparing the standard model cross section with and without the  $Z^0$  exchange. For  $\theta_{\min}$  as large as  $\pi/6$ , the  $Z^0$  contribution is only 3%-4% of the total. The result scales approximately as the logarithm of  $\eta$ , and we use  $\eta = 10^{-5}$  in the figures.

To complete the calculation of the cross section for the  $e\gamma$  process, it is necessary to fold the cross section, Eq. (12), with the distribution  $F_\gamma(x)$  of backscattered photons having momentum fraction  $x$  [9] to obtain

$$\sigma_T = \frac{1}{s} \int_{m_A^2}^{0.83s} d\hat{s} F_\gamma(\frac{\hat{s}}{s}) \sigma_{e\gamma \rightarrow eA^0}(\hat{s}) , \quad (13)$$

with  $\hat{s} = xs$ . Here, we have taken the usual upper limit on the allowed  $x$  value,  $x = 0.83$ .

This cross section is plotted in Fig. (1) for  $M\mu > m_W^2 \sin 2\beta$  and in Fig. (2) for  $M\mu < m_W^2 \sin 2\beta$ . The dashed line in each panel is the contribution from the top and bottom quarks and the tau lepton. For large  $\tan \beta$ , the tau contribution is important. This is illustrated in the  $\tan \beta = 20$  panel of Fig. (1), where the dot-dashed line is the contribution from the top and bottom quarks. In Fig. (1), the solid lines are  $m_1 = 250$  GeV and  $m_2$  the largest value consistent with the constraint  $(m_1 - m_2) \geq m_W \sqrt{2(1 + \sin 2\beta)}$ , which is needed to ensure that  $M$  and  $\mu$  are real. Similarly, in Fig. (2), the solid lines correspond to  $m_1 = 250$  GeV and  $m_2$  the largest value consistent with  $(m_1 - m_2) \geq m_W \sqrt{2(1 - \sin 2\beta)}$ . Unlike the  $M\mu > m_W^2 \sin 2\beta$  case, when  $M\mu < m_W^2 \sin 2\beta$  it is possible for  $m_1$  and  $m_2$  to be equal for  $\tan \beta = 1$  provided the  $m_1, m_2 \geq m_W$ . These values of  $m_1$  and  $m_2$  are within the range of chargino masses found in studies of minimal supersymmetric models [10]. In most cases, the inclusion of the chargino contribution leads to a significant increase in the cross section, especially for the larger values of  $\tan \beta$ .

To assess the observability of this process, we assume that the dominant  $A_0$  decay is  $A_0 \rightarrow b\bar{b}$ . For  $m_A < 2m_t$ , this ignores some contribution from chargino pair decay, but this is relatively small since in all but one of the examples we consider the lowest chargino mass exceeds  $\sim 120$  GeV. Even above the top threshold,  $b\bar{b}$  decay dominates when  $\tan \beta \sim 20$  [11]. The dotted lines in Figures (1) and (2) are the cross section for the direct production of a background  $b\bar{b}$  of invariant mass  $m_A$  in  $e\gamma$  collisions subject to an angular cut on the  $b$  and  $\bar{b}$  direction relative to the that of the incident photon in the  $e\gamma$  center of mass. We find that an angular cut of  $|\cos \theta| < .98$  on both the  $b$  and the  $\bar{b}$  reduces the background  $b\bar{b}$  cross section by about a factor of 10 while leaving the  $b\bar{b}$  signal from  $A^0$  decay essentially unchanged. More restrictive cuts on the  $b$  and  $\bar{b}$  angles can further suppress the background, but at the expense of a significant decrease in the signal [12]. The cut shown appears to be

optimal.

### III. DISCUSSION

We would like to point out that the  $e\gamma$  cross sections calculated here are very likely to be much larger than those of the related process  $e\bar{e} \rightarrow \gamma A^0$  at 500 GeV. We have checked this for the production of the standard model Higgs-boson using the complete (standard model) calculation of  $e\bar{e} \rightarrow \gamma H^0$  [7] and the photon pole contribution to  $e\gamma \rightarrow eH^0$ . At an  $e\bar{e}$  center of mass energy of 500 GeV, we find the cross section  $\sigma(e\bar{e} \rightarrow \gamma H^0)$  for the production of a 200 GeV  $H^0$  is 0.08 fb, whereas  $\sigma(e\gamma \rightarrow eH^0) = 5.9$  fb for the same Higgs-boson mass.

This enhancement is implicit in a previous calculation of scalar Higgs-boson production [8]. In Ref. [8], the Weizsäcker-Williams approximation is used for the  $t$  channel photon together with the on-shell  $H \rightarrow \gamma\gamma$  amplitude. This is essentially equivalent to setting  $y = 0$  in the parentheses of Eq. (12) and using  $m_e^2$  as the cutoff in the remaining integral [13]. Our comparison of the approximate results of Ref. [8] with an exact calculation suggests that the Weizsäcker-Williams approach tends to overestimate the cross section. Apart from minor variations depending on how the calculation is performed, it is nevertheless true that the  $t$  channel cross section is substantially larger than its  $s$  channel counterpart.

The production of  $A^0$  has also been investigated in  $\gamma\gamma$  collisions [14]. In this case, the background arises from the process  $\gamma\gamma \rightarrow b\bar{b}$  and it is effectively suppressed by imposing an angular cut. With our choice of chargino masses, a comparison of the  $\tan\beta = 20$  cross sections in  $e\gamma$  production and  $\gamma\gamma$  production [14] reveals a larger signal in the  $e\gamma$  mode. Both channels are likely to be important in searches for the  $A^0$ .

To the extent that the photon pole contribution can be isolated, this method of searching for the  $A^0$  has the advantage that the contributions from supersymmetry are significant and limited to one type supersymmetric particle. Should one observe a cross section larger than any standard model prediction, the case for the presence of chargino contributions is rather

strong.

#### **ACKNOWLEDGMENTS**

We would like to acknowledge conversations with C.-P. Yuan and X. Tata. This research was supported in part by the National Science Foundation under grant PHY-93-07980 and by the United States Department of Energy under contract DE-FG013-93ER40757.

## REFERENCES

- [1] *The Higgs Hunter's Guide*, J. F. Gunion, H. E. Haber, G. Kane and S. Dawson, Addison-Wesley Publishing Company, 1990.
- [2] The same thing can be said about the production of scalar Higgs-bosons in the reaction  $e\gamma \rightarrow e H^0$ .
- [3] J. F. Gunion and H. W. Haber, Nuc. Phys. **B272**, 1 (1986).
- [4] H. Baer, A. Bartl, D. Karatas, W. Majerotto, and X. Tata, Int. J. Mod. Phys. **A4**, 4111 (1989) Appendix B.
- [5] X. Tata and D. A. Dicus, Phys. Rev. D **35**, 2110 (1987).
- [6] G. 't Hooft and M. Veltman, Nuc. Phys. B **153**, 365 (1979).
- [7] A. Abbasabadi, D. Bowser-Chao, D. A. Dicus and W. W. Repko, Phys. Rev D **52**, 3919 (1995).
- [8] O. J. P. Éboli, M. C. Gonzalez-Garcia and S. F. Novaes, Phys. Rev. D **49**, 91 (1994).
- [9] I. F. Ginzburg, G. L. Kotkin, S. L. Panfil, V. G. Serbo, and V. I. Telnov, Nucl. Instrum. Methods **219**, 5 (1984).
- [10] G. L. Kane, C. Kolda, L. Roszkowski, and J. D. Wells, Phys. Rev. D **49**, 6173 (1994).
- [11] V. Barger, K. Chung, R. J. N. Phillips, and A. L. Strange, Phys. Rev. D **46**, 4914 (1992).
- [12] If the  $A^0$  mass should turn out to be very close to the  $Z$  mass, there could be a substantial background from  $\gamma e \rightarrow Z e \rightarrow b\bar{b} e$ . We have not included this in our background calculation.
- [13] To see this in detail, compare the simplified Eq. (12) with Eq. (4) of Ref. [8].
- [14] J. F. Gunion and H. E. Haber, Phys. Rev. D **48**, 5109 (1993).

## FIGURES

FIG. 1. Cross sections for the production of  $A^0$  are shown for various values of  $\tan\beta$  and an  $e\bar{e}$  center of mass energy of 500 GeV when  $M\mu > m_W^2 \sin 2\beta$ . In each case, the solid line corresponds to chargino masses  $m_1 = 250$  GeV and  $m_2$  the largest value consistent with the restriction  $(m_1 - m_2) \geq m_W \sqrt{2(1 + \sin 2\beta)}$ . The dashed line is the standard two Higgs doublet contribution without charginos, and the dot-dashed line in the  $\tan\beta = 20$  panel is the two Higgs doublet result without the  $\tau$  contribution. The dotted lines are the cross section for the production of a background  $b\bar{b}$  with invariant mass  $m_A$ . In these graphs, the angular cutoff  $\eta$  is taken to be  $10^{-5}$ .

FIG. 2. Same as Fig. (1) for  $M\mu < m_W^2 \sin 2\beta$ . In this case,  $m_1$  and  $m_2$  satisfy the condition  $(m_1 - m_2) \geq m_W \sqrt{2(1 - \sin 2\beta)}$ .

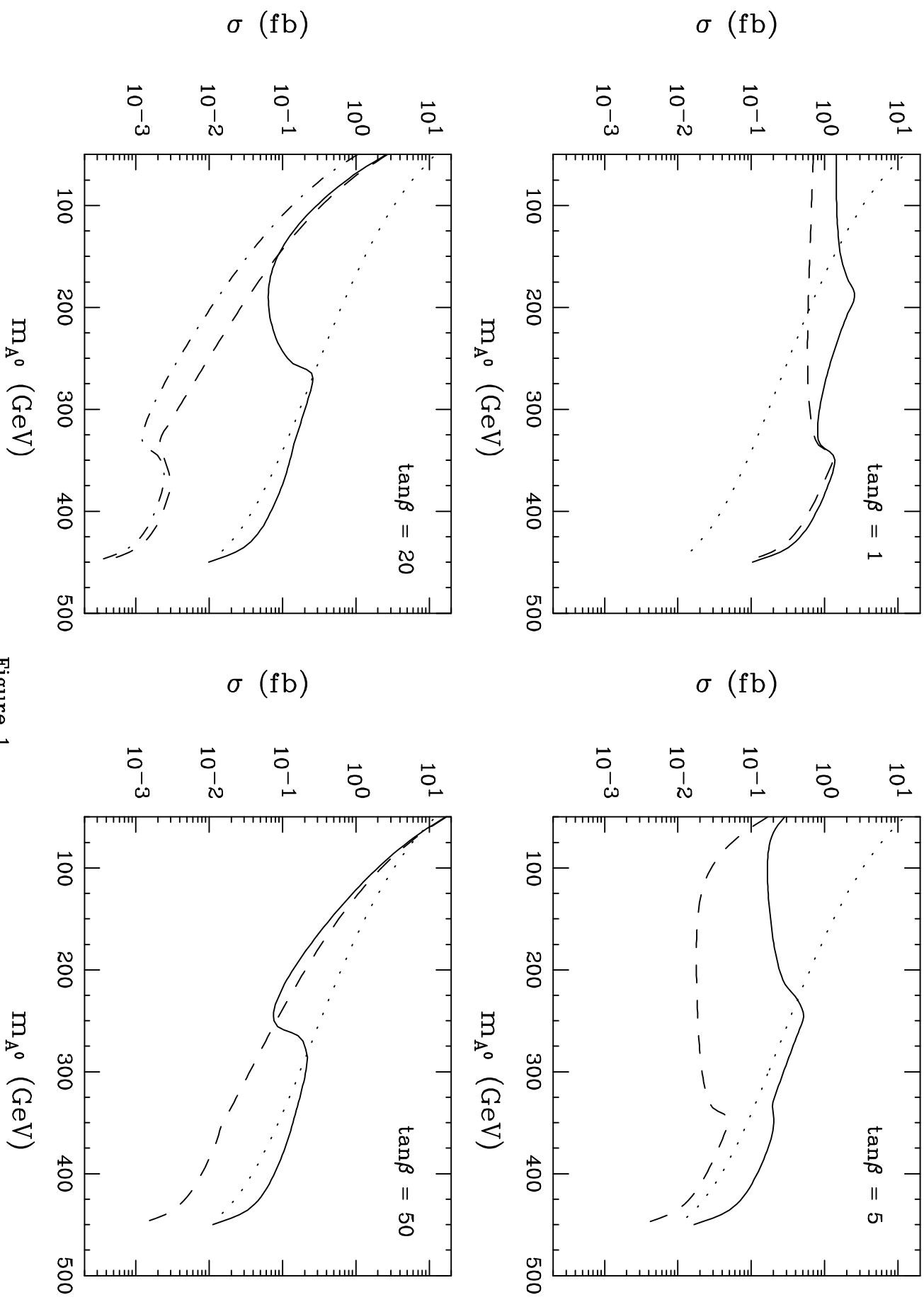


Figure 1

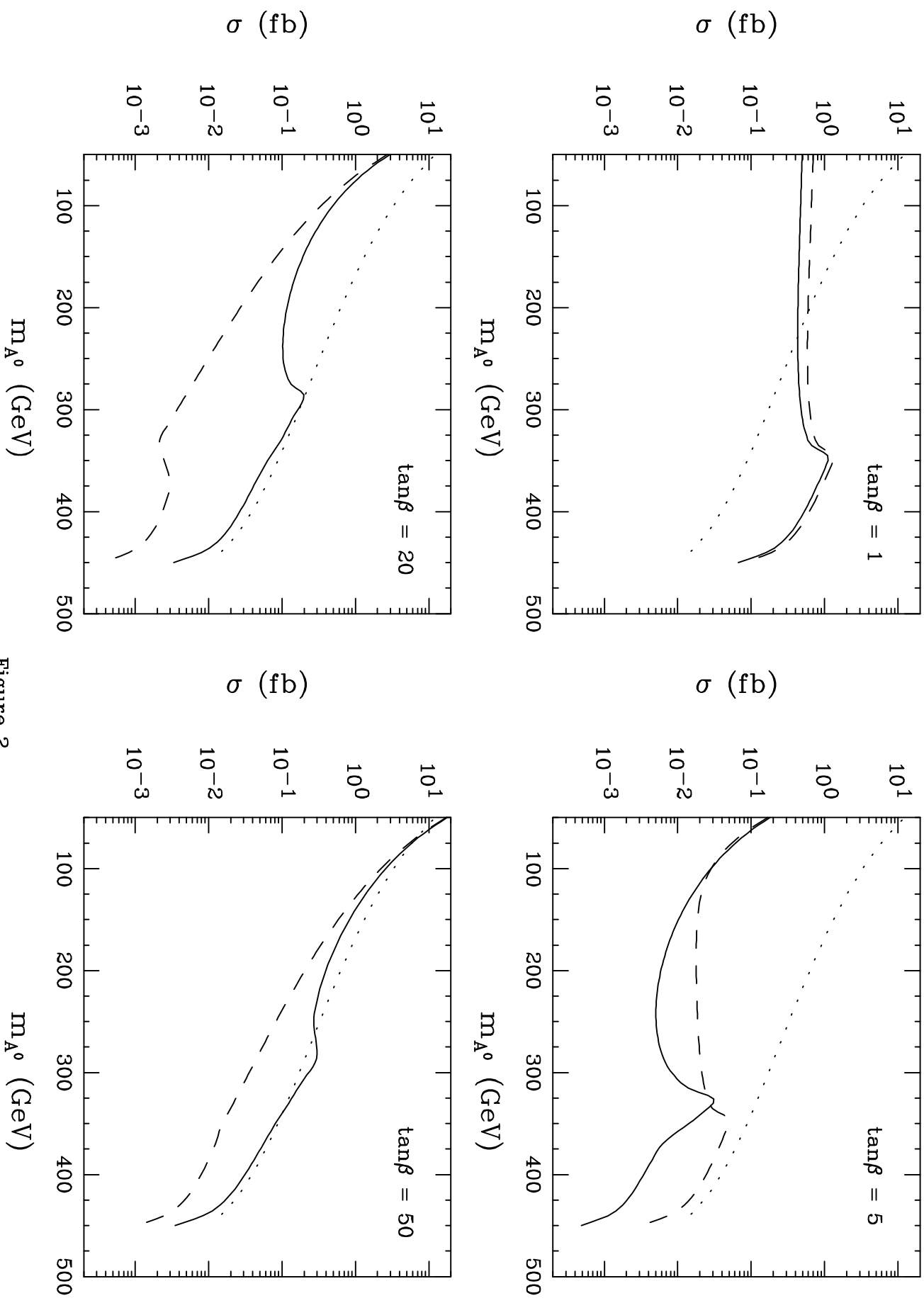


Figure 2